arXiv:1606.08915v3 [cond-mat.str-el] 18 Aug 2016

Unconventional Tomonaga-Luttinger Liquid Exponents in Dirac Materials

Matthew P. Gochan[1] and Kevin S. Bedell[1]

[1] *Department of Physics, Boston College, Chestnut Hill, Massachusetts 02467, USA*

(Dated: August 19, 2016)

Dirac materials are systems in which the dispersion is linear in the vicinity of the Dirac points. As a consequence of this linear dispersion, these systems exhibit unusual behavior and possess unique physical properties that are of great interest. In this work we utilize the single walled carbon nanotube (SWNT) as a model Dirac material and examine the system within the framework of Tomanaga-Luttinger Liquid theory (TLL) revealing several unconventional properties unique to these systems. Specifically, the exponents of the Green's function are electron density independent leading to electron density independent thermodynamic quantities and speed of sound; both of which are vastly different from traditional TLL behavior. Additionally, we discuss the implications the Virial Theorem has for this system; in particular, the total average ground state energy is given by $E = \mathcal{B}/r_s$ where $\mathcal{B}$ is a constant independent of r_s. Finally, experimental techniques are discussed in which these predictions of density independent exponents and their behavior can be verified.

PACS numbers: 73.22.Pr, 71.10.Pm

I. INTRODUCTION

Dirac materials encompass a large family of materials that are at the forefront of theoretical and experimental research. Graphene, topological insulators, and d-wave superconductors are a few examples in this family that have been thoroughly studied and exhibit new results and rich physics. These examples, in spite of being different, share a fundamental similarity that links them together: their low energy fermionic excitations behave as massless Dirac particles [1]. A standard tight-binding calculation immediately leads to an exact linear dispersion in the vicinity of the Dirac points and is vastly different from the parabolic dispersion found in ordinary systems. Thus, any properties that are a direct consequence of this linear spectrum are universal among these diverse materials. For example, the fermionic specific heat is controlled by the linear behavior and its power law dependence is shared by graphene, d-wave superconductors, and superfluid ^{3}He. In addition to these low energy properties, some Dirac materials are also boundary states for exotic quantum phases and have drawn great research interest. Specifically, the so-called Dirac semi-metal can be driven into various quantum states such as Weyl semimetals, axion insulators, and topological superconductors [2]. Although Dirac materials possess different properties. It is the universal low energy behavior, the possibility of realizing exotic quantum states of matter, and the rich fundamental physics within Dirac materials that has fueled the research into understanding these systems.

The system under consideration is a single walled carbon nanotube in its metallic state and at $T = 0$. We avoid other chiralities to stay away from gapped states and avoid possible Wigner crystalliztion [3, 4]. It's effectively a one dimensional Dirac material. As a consequence of this reduced dimensionality, Fermi Liquid theory is no longer valid and Tomanaga-Luttinger Liquid theory is necessary to describe the low-energy asymptotic behavior [5, 6]. The Hamiltonian for a SWNT using TLL theory has the following form (we set $\hbar = 1$ for the remainder of the letter)[5]

$$H = H_0 + H_{int} \tag{1}$$

where H_0 is the Hamiltonian for a free Dirac gas:

$$H_0 = v_g \sum_{r,k,\sigma} (rk - k_F)\, c^{r\dagger}_{k\sigma} c^{r}_{k\sigma} \tag{2}$$

and H_{int} is the Tomanaga-Luttinger interaction [7]:

$$\begin{aligned} H_{int} = \frac{1}{L} \sum_{k_1,k_2,p,\alpha,\beta} \Big[& \Gamma^2_{\alpha,\beta} c^{+\dagger}_{k_1,\alpha} c^{-\dagger}_{k_2,\beta} c^{-}_{k_2+p,\beta} c^{+}_{k_1-p,\alpha} \\ & + \frac{1}{2}\Gamma^4_{\alpha,\beta} \Big(c^{+\dagger}_{k_1,\alpha} c^{+\dagger}_{k_2,\beta} c^{+}_{k_2+p,\beta} c^{+}_{k_1-p,\alpha} \\ & + c^{-\dagger}_{k_1,\alpha} c^{-\dagger}_{k_2,\beta} c^{-}_{k_2+p,\beta} c^{-}_{k_1-p,\alpha} \Big) \Big] \end{aligned} \tag{3}$$

where the Fermi velocity $v_g \sim 10^6$ m/s is a constant, $r = +, -$ denotes whether the electrons are right or left movers respectively, and $c^\dagger, c$ are the creation and annihilation operators for fermions. $\Gamma^i_{\alpha,\beta} = g^s_i \delta_{\alpha,\beta} + g^a_i \delta_{\alpha,-\beta}$ $(i = 2, 4)$ describes the interaction between electrons; $i = 2$ refers to forward scattering between electrons on separate branches while $i = 4$ refers to forward scattering between electrons on the same branch. The superscripts s and a denote symmetric and anti-symmetric spin respectively. The coupling constants, g^s_i and g^a_i, are a measure of the interaction strength between electrons for given scattering processes and are in general momentum dependen; we neglect this dependence by restricting the momentum to within certain values Λ [5]. The interaction given in (3) only contains terms involving forward scattering; Umklapp and back scattering processes have been ignored. This exclusion is justified through the following: as long as we're considering low-energy properties, interactions that don't commute with charge and spin separation are irrelevant [6].

We immediately notice an important distinction in (2) that isn't seen in conventional 1D metals; although TLL theory produces exact results for the Green's function in the vicinity of the fermi points ($\pm k_F$), the result is hinged upon the linearity of the dispersion relation [8, 9]. In ordinary 1D metals, this linear behavior is obtained by linearizing the quadractic dispersion around $\pm k_F$ and is therefore only exact in a region within a momentum cutoff (e.g. $k_F - \Lambda < k < k_F + \Lambda$). In Dirac materials, the linear behavior exists naturally without linearization leading to validity for all k.

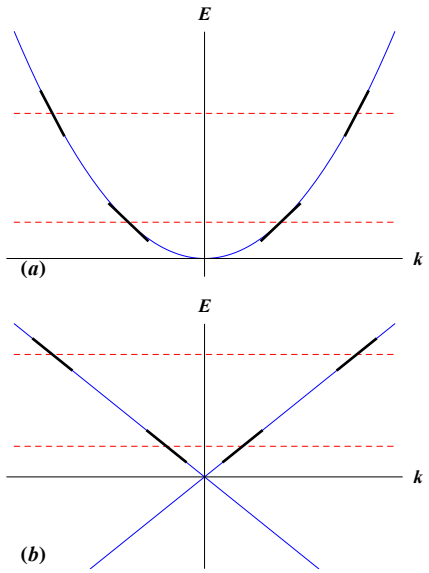

FIG. 1: (color online) (a) The dispersion for a normal 1D metal. The red dashed lines denote different values for the Fermi energy. Notice how the linearization at different k_F points (i.e. different density) produces different slopes (black lines) and therefore different values for v_F. (b) The dispersion for a 1D Dirac metal. No matter where the Fermi energy is, the slope, and therefore v_F, is the same.

Dzyaloshinskii and Larkin have shown [10] that a simple expression for the Green's function exists in real space and time for the Tomanaga-Luttinger model. Mimicking their procedure, the Green's function for a SWNT is found to be

$$G_r(x,t) = \frac{1}{2\pi}\frac{rx - v_g t + i/\Lambda}{rx - v_g t + i\delta}\times \prod_{j=\sigma,\rho}\frac{1}{(rx - u_j t + i/\Lambda)^{1/2}}\times \frac{1}{\left[\Lambda^2\left(x^2 - u_j^2 t^2 + \frac{i}{\Lambda}\left(2u_j t - \frac{i}{\Lambda}\right)\right)\right]^{\alpha_j}} \tag{4}$$

where δ is the bandwidth cutoff and Λ is the momentum transfer cutoff. u_σ and u_ρ have the following form:

$$u_\sigma^2 = \left[v_g + \frac{1}{2\pi}\left(g_4^s - g_4^a\right)\right]^2 - \left[\frac{1}{2\pi}\left(g_2^s - g_2^a\right)\right]^2 \tag{5a}$$

$$u_\rho^2 = \left[v_g + \frac{1}{2\pi}\left(g_4^s + g_4^a\right)\right]^2 - \left[\frac{1}{2\pi}\left(g_2^s + g_2^a\right)\right]^2 \tag{5b}$$

The exponents, α_σ and α_ρ, are of special interest and have the following form:

$$\alpha_\sigma = \frac{1}{4u_\sigma}\left[v_g + \frac{1}{2\pi}\left(g_4^s - g_4^a\right) - u_\sigma\right] \tag{6a}$$

$$\alpha_\rho = \frac{1}{4u_\rho}\left[v_g + \frac{1}{2\pi}\left(g_4^s + g_4^a\right) - u_\rho\right] \tag{6b}$$

It is within these exponents that we start to see a deviation from traditional TLL behavior.

α_σ and α_ρ are a measure of interaction strength in the system and are the signature of TLL behavior. They appear in numerous thermodynamic quantities in ways that differentiate them from Fermi Liquid behavior. In a normal 1D metal the exponents take the following form [5]

$$\alpha_\sigma = \frac{1}{4u_\sigma}\left[v_F + \frac{1}{2\pi}\left(g_4^s - g_4^a\right) - u_\sigma\right]$$

$$\alpha_\rho = \frac{1}{4u_\rho}\left[v_F + \frac{1}{2\pi}\left(g_4^s + g_4^a\right) - u_\rho\right]$$

In comparing the above expressions to those in (6a) and (6b), the only difference between the exponents in a normal metal and a Dirac material is the Fermi velocity. In a normal metal, v_F depends linearly on electron density; in a Dirac material, v_g is a constant and is the velocity of all electrons throughout the system; see FIG. 1.

This difference has immediate consequences in regards to the interaction strength in the 1D Dirac material. Since (6a) and (6b) are density independent, the strength of the interactions in this system is a constant regardless of the number of particles in the system. Additionally, the constant velocity in the exponents reveals more unique behavior that distances SWNTs and other 1D Dirac materials from a TLL in profound ways thus hinting at a new class of 1D materials.

From (4) we can immediately derive the momentum distribution function as done in [11].

$$n(k) = -i\sum_r \int_{-\infty}^{\infty} G_r(x, 0^-)e^{-ikx}dx \tag{7}$$

The integral in (7) is solvable in the vicinity of the fermi points ($k \approx k_F$) and leads to the following expression:

$$n(k) \simeq \frac{1}{2} - C_1\left|k - rk_F\right|^\alpha \operatorname{sgn}\left(rk - k_F\right) - C_2\left(k - rk_F\right) \tag{8}$$

where $\alpha = 2(\alpha_\sigma + \alpha_\rho)$ and the constants C_1 and C_2 have the following form:

$$C_1 = \frac{\Gamma\left(\frac{1}{2} - \alpha_\sigma - \alpha_\rho\right)}{2\pi^{1/2}\Gamma\left(1 + \alpha_\sigma + \alpha_\rho\right)}\left(\frac{\Lambda}{2}\right)^{\alpha} \tag{9a}$$

$$C_2 = \frac{\beta\left(\frac{1}{2}, \alpha_\sigma + \alpha_\rho - \frac{1}{2}\right)}{2\pi}\Lambda \tag{9b}$$

where $\Gamma(x)$ and $\beta(a,b)$ are the gamma and beta function respectively [12]. This momentum distribution function has a number of interesting features. First, we see the non-Fermi Liquid like behavior in $n(k)$. If a SWNT behaved as a Fermi Liquid, then $n(k)$ would have a singularity at $k = k_F$. The expression (8) obtained is continuous for all k is a trademark of TLL behavior. Second, we see a singularity in the derivative, $\frac{dn}{dk}$, at $k = \pm k_F$. This indicates the quasi-particle picture failing in TLL systems.

Recent angle resolved photoemission spectroscopy (ARPES) measurements performed on SWNTs have exposed behavior consistent with TLL theory [13]. Such behavior, which is vastly different from traditional Fermi-liquid Theory behavior, was seen in the spectral function and intensities which both exhibit the desired power-law behavior in good agreement with theory. These results motivated our investigation of SWNTs within TLL theory and lead to the main question: will the unusual behavior of Dirac electrons in SWNTs lead to possible deviations from TLL behavior? As we will see, a number of non-trivial results emerge in SWNTs that aren't seen in ordinary 1D metals.

This paper is outlined as follows: First we derive the density of states of a SWNT near the Dirac points, and the thermodynamic quantities of the system. Next, we derive the total ground state energy of the system and discuss the implications of the expression as well as the apparent connection to Coulomb systems. Next, we discuss possible experiments that can test our predictions. Finally, we have concluding remarks.

II. DENSITY OF STATES

With the momentum distribution (8), we derive the density of states:

$$g(E) = \frac{1}{L}\frac{dN}{dE}$$

where L is the length of the SWNT and N is the number of electrons given by:

$$N = \frac{L}{2\pi}\int n(k)dk$$

We limit ourselves to a small area, δk, around $\pm k_F$ where eqn. (8) is valid. In this area, small changes in N with respect to k can be expressed as:

$$\frac{\delta N}{\delta k} = \frac{L}{2\pi}\left(1 - \frac{C_1}{\alpha+1}(\delta k)^{\alpha} + \frac{C_2}{2}\delta k\right)$$

In the limit as $\delta k \to 0$, the δk term is negligible since $0 < \alpha < 1$ [13, 14]. Finally, we obtain the density of states of a SWNT near the Fermi points:

$$g(\omega) = \frac{2}{\pi v_g}\left(1 - \frac{C_1}{v_g^{\alpha}(\alpha+1)}|\omega|^{\alpha}\right) \tag{10}$$

where C_1 is defined in (9a) and ω is measured from the Fermi points. Our expression is consistent with the ARPES results in [13] that obtain $g(\omega) \sim |\omega|^{\alpha}$. Additionally, (10) reduces to the expression for the density of states for a non-interacting 1D Dirac system ($\alpha = 0$).

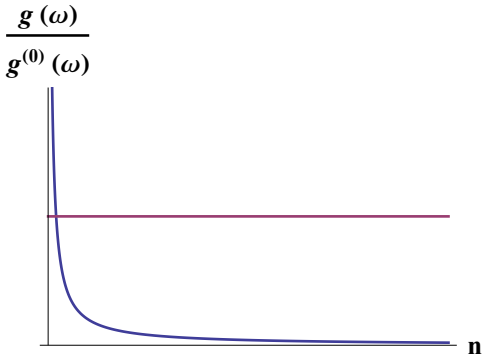

FIG. 2: (color online) Plot of density of states normalized to the non-interacting value as a function of electron density. The blue curve represents $g/g^{(0)}$ for a normal metal while the purple line represents $g/g^{(0)}$ for a Dirac system. We see a clear distinction in the behavior of the density of states between the systems indicating that the dimensionality of the system, although important, isn't nearly as important as the behavior of the dispersion.

The interesting feature of eqn. (10) is due to the velocity term. As we saw in Fig. 1, the velocities between a normal 1D metal and 1D Dirac metal are very different. This different dispersion is responsible for the unique behavior of $g(\omega)$ that can be seen in Fig. 2 and Fig. 3; constant behavior as opposed to the traditional hyperbolic behavior. A consequence of this density independence is an apparent saturation in the number of eigenstates of the system. Additionally, since $g(\omega)$ is density independent, thermodynamic quantities in 1D Dirac systems also exhibit density independence.

A. Thermodynamic Quantities

Various thermodynamic quantities exhibit unusual behavior that is of interest. Although exressions for these quantities can be obtained through (8) and (10), we turn to bosonization for a richer and more elegant derivation. Normal metals, those with parabolic dispersion, in 1D have been extensively studied using bosonizataion [15–18]; here, we apply such techniques to a SWNT. The bosonized Hamiltonian has the following form:

$$H = H_\rho + H_\sigma \tag{11}$$

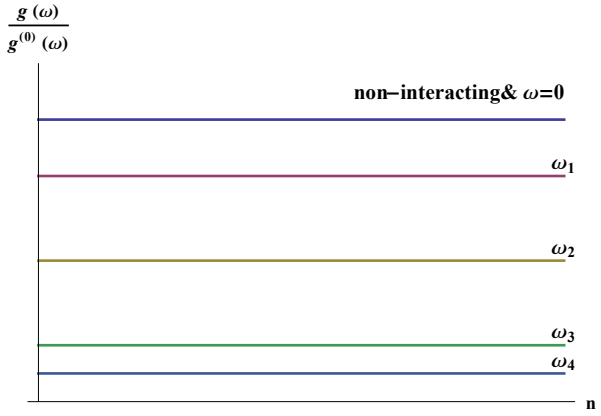

FIG. 3: (color online) Plot of density of states normalized to the non-interacting value as a function of electron density n for various values of ω. As we get further away from the Fermi points, the value of $g(\omega)$ decreases but remains constant for all density.

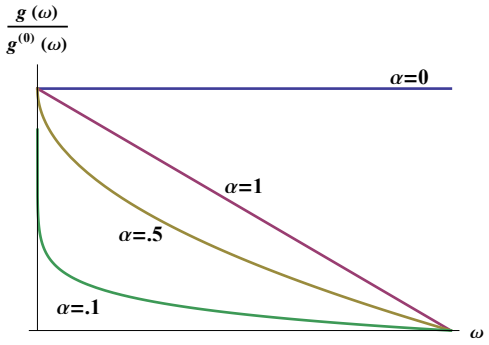

FIG. 4: (color online) Plot of density of states normalized to the non-interacting value as a function of frequency for various values of α ([13] obtained $\alpha = 0.46 \pm 0.10$). In the presence of interactions ($\alpha \neq 0$), $g(\omega)$ behaves very differently from its non-interacting expression. We see from the above figure the predicted suppression of the density of states is seen in both normal metals and Dirac systems; $g/g^{(0)} \to 0$ as ω increases.

which clearly shows the separation of charge and spin that's seen in 1D Fermi systems. These two independent boson modes give rise to the following dispersions:

$$\varepsilon_i = u_i k \qquad i = \rho, \sigma \tag{12}$$

where u_ρ and u_σ are defined by (5a) and (5b). In the absence of a magnetic perturbation and the presence of a charge perturbation, the charge density mode propagates and gives rise to the speed of sound:

$$v = v_g \sqrt{1 + \frac{2g_4}{v_g \pi} + \frac{1}{(v_g \pi)^2}\left[(g_4)^2 - (g_2)^2\right]} \tag{13}$$

where we set $g_i = g_i^s = g_i^a$ based on anti-symmetry arguments. The speed of sound can also be obtained from the chemical potential as shown in [19]. Both expressions are in agreement which shows we haven't missed any of the Hilbert space working in the boson representation [17]. In the weak coupling limit, we can neglect terms quadratic and higher in the coupling constant to obtain:

$$v = v_g \sqrt{1 + \frac{2g_4}{v_g \pi}} \tag{14}$$

which is the same expression obtained in [10]. Both expressions for the speed of sound, (13) and (14), have the density independent behavior that's the main point of this letter. Density independent speed of sound is surprising due to its counter-intuitive nature. Speed of sound (first sound in the Landau and Lifshitz language [20]) is understood as a wave of compression and rarefaction. With an increase in electron density, one would expect a change in the speed of sound yet our result shows otherwise.

With the dispersion in (12), we can calculate all thermodynamic quantities. For example, the specific heat:

$$C_v(T) = \left[\frac{\pi k_B^2}{3}\left(\frac{1}{u_\sigma} + \frac{1}{u_\rho}\right)\right] T \tag{15}$$

(15) has a linear dependence in temperature, which is characteristic of both fermi and bose systems at low temperature. However, the difference appears in the constant multiplying T in (15). For typical 1D fermi systems, the constant will depend inversely with density; in a SWNT the constant has a fixed value regardless of density. Thus the specific heat is also density independent. Other quantities such as the spin susceptibility, compressibility, and conductivity can be derived using the bosonic dispersions [5, 6, 17] and all present this density independence that's unique to 1D Dirac materials. In general, we conclude that due to the density independence in (10), all thermodynamic quantities will themselves be independent of density; in spite of the contradiction to conventional physical interpretation.

III. AVERAGE GROUND STATE ENERGY

Recent work on Dirac materials in the presence of a Coulomb potential using the Virial Theorem provides an expression for the average ground state energy of the system [21]:

$$E\left(r_s\right) = \frac{\mathcal{B}}{r_s} \tag{16}$$

where $\mathcal{B}$ is a constant independent of density. In this paper, r_s is a dimensionless constant that's a measure of density. Specifically, r_s allows us to express the electron spacing in units of a characteristic length of the system; in this case, we have $r = ar_s$ where a is the characteristic length. Although the work in [21] was done for 2D, the form for (16) remains the same regardless of the dimension of the system; the only thing that changes with

a change in dimension is the constant $\mathcal{B}$. Therefore, we expect the average ground state energy of a SWNT to have the same form as (16).

We start with an expression relating the compressibility of the system to the average ground state energy:

$$\kappa^{-1} = n^2 \frac{\partial^2 \mathcal{E}}{\partial n^2} \tag{17}$$

where we define the energy density $\mathcal{E} = E/l$. The benefit in using (17) is the following: in 1D, the expression $n^2\kappa$ is independent of density. This allows for a straightforward integration of (17) to obtain $\mathcal{E}$:

$$\mathcal{E} = \frac{1}{2}\kappa^{-1} \tag{18}$$

where the compressibility for a 1D system with Dirac spectrum is $\kappa = 4v_g/\pi n^2 v^2$ where v is given by (14). The total average ground states energy is then:

$$E\left(r_s\right) = \frac{N\pi v_g}{8a}\left(1 + \frac{2g_4}{\pi v_g}\right)\frac{1}{r_s} \tag{19}$$

where $a = 1.44$ Å[19, 22]. The term in front of $1/r_s$ is

$$\frac{\mathcal{B}}{N} = \frac{\pi\hbar v_g}{8a}\left(1 + \frac{2g_4}{\pi v_g}\right) \tag{20}$$

(where $\hbar$ has been restored) and, as expected, is independent of r_s. For a typical SWNT, $\frac{\mathcal{B}}{N} \approx 2.8 \pm .2$ eV.

The result for the energy (19) is nontrivial and has a few remarkable consequences: first, there seems to be a connection between the Tomanaga-Luttinger system and a Coulomb system. These systems are vastly different, specifically in their interaction potentials, yet their average ground state energies have the same form and dependence on r_s, with the exception that the constant $\mathcal{B}$ will be a different number. Such a similarity alludes to the specific form of the potential not being important; but rather the exact linear dispersion controls the physics. Second, a closed form for the ground state energy (19) provides a bound allowing calculation of many quantities for the SWNT. This closed form for the ground state energy is a rare thing that appears in all Dirac materials [21].

IV. EXPERIMENTAL REALIZATION

In order to test the density independent behavior predicted in this letter, we need scanning tunneling microscopy (STM). With STM, data for the density of states can be obtained through [23]:

$$\text{DoS} \propto \frac{dI}{dV} \approx V^{\alpha} \tag{21}$$

where α has the same meaning as before, V is the voltage, and I is the current. Although many STM experiments have been done before on SWNTs, none had the goal of testing the density independence; previous experiments were focused on imaging and the dependence of the chiral indices on the density of states. In a sense, testing for this density dependence is easier than previous experiments due to the lifting of the uniformity requirement; we want multiple SWNTs with varying density. With that in mind, we expect the dI/dV plots to remain independent of density. Prior experiments [13, 14] have observed the temperature dependence of the differential conductance and have obtained good agreement with the theory. We would like to see results for keeping the temperature constant, and low, while changing the eletron density. We expect results similar to what can be seen in Fig. 3. In addition to revealing the density dependence in SWNTs, an experiment like this has the added bonus of re-affirming the existence of Luttinger-Liquid like states. Past experiments have been in agreement with theory, yet skeptics believe the observed behavior to be circumstantial due to the confined dimension of the electrons [3]. Data from the proposed experiment testing density dependence would help solidify the idea that these states exist. Additionally, thermodynamic quantities (e.g. the specific heat) of SWNTs can be obtained at varying densities, with all other things constant, and should be the same value indicative of this electron density independent behavior.

V. CONCLUSION

In this letter we have demonstrated that the exact linear dispersion and the constant Fermi velocity found in Dirac materials gives rise to nontrivial physics. While we observe typical Tomanaga-Luttinger Liquid behavior in the continuous momentum distribution function and low energy density of states, there are also profound differences. For example, the density independent exponents and subsequent density independent physical quantities, such as the specific heat and speed of sound, are differences that are unique to Dirac materials. Such vast differences hint at a new class of 1D systems called Dirac liquids as opposed to Tomonaga-Luttinger liquids. From studying these Dirac liquids we have a deeper understanding of the physics contained within Dirac materials; specifically, the importance of interactions in the system, and the importance of dimensionality. Additionally, a strange similarity between TLL systems and Coulomb systems emerges that hints at the linearity of the dispersion, rather than the specific potential, as being more important in the unusual observed properties. From here, we hope to use this work to shed light on even more exotic Dirac materials such as Weyl semimetals and topological Dirac semimetals. Such materials are predicted to be stable bulk analogs of graphene, as well as a playground for relativistic effects. As such, Dirac materials are a unique and exciting class of materials that possess rich physics as well as promise for technological advancement.

VI. ACKNOWLEDGMENTS

The authors, M.P. Gochan and K.S. Bedell, would like to thank Thomas Mion and Dr. Ilija Zeljkovic for valuable discussion in regards to experimental techniques as well as James Stokes, Dr. Robert Konik, and Dr. Alexander Balatsky, for fruitful discussion. Additionally, we thank the IMS at LANL for their hospitality. This work was supported in part by the John H. Rourke, Boston College, Endowment Fund and the NSF Grant PHY-1208521

[1] T. O. Wehling, A. M. Black-Schaffer, and A. V. Balatsky, Advances in Physics **63**, 1 (2014), 1405.5774.
[2] Z. Liu, J. Jiang, B. Zhou, Z. Wang, Y. Zhang, H. Weng, D. Prabhakaran, S. Mo, H. Peng, P. Dudin, et al., Nature materials **13**, 677 (2014).
[3] V. V. Deshpande, M. Bockrath, L. I. Glazman, and A. Yacoby, Nature **464**, 209 (2010).
[4] V. V. Deshpande and M. Bockrath, Nature Physics **4**, 314 (2008).
[5] J. Sólyom, Advances in Physics **28**, 201 (1979).
[6] J. Voit, Journal of Physics: Condensed Matter **5**, 8305 (1993).
[7] K. B. Blagoev and K. S. Bedell, Phys. Rev. Lett. **79**, 1106 (1997).
[8] S. I. Tomonaga, Progress of Theoretical Physics **5**, 544 (1950).
[9] J. M. Luttinger, Journal of Mathematical Physics **4**, 1154 (1963).
[10] I. E. Dzyaloshinskii and A. I. Larkin, Journal of Experimental and Theoretical Physics **41**, 202 (1974).
[11] J. Voit, Reports on Progress in Physics **58**, 977 (1995).
[12] I. S. Gradshteyn and I. M. Ryzhik, *Table of integrals, series, and products* (Elsevier/Academic Press, Amsterdam, 2007), seventh ed.
[13] H. Ishii, H. Kataura, H. Shiozawa, H. Yoshioka, H. Otsubo, Y. Takayama, T. Miyahara, S. Suzuki, Y. Achiba, M. Nakatake, et al., Nature **426**, 540 (2003).
[14] M. Bockrath, D. H. Cobden, J. Lu, A. G. Rinzler, R. E. Smalley, L. Balents, and P. L. McEuen, Nature **397**, 598 (1999).
[15] G. D. Mahan, *Many-particle physics* (Springer Science & Business Media, 2013).
[16] P. Phillips, *Advanced Solid State Physics*, Advanced Book Program (Westview Press, 2003).
[17] T. Giamarchi, *Quantum Physics in One Dimension*, International Series of Monographs on Physics (Clarendon Press, 2003).
[18] A. Gogolin, A. Nersesyan, and A. Tsvelik, *Bosonization and Strongly Correlated Systems* (Cambridge University Press, 2004).
[19] P. Nozieres and D. Pines, *Theory Of Quantum Liquids*, Advanced Books Classics Series (Westview Press, 1999).
[20] L. Landau, E. Lifshits, and L. Pitaevskiĭ, *Statistical Physics*, no. pt. 2 in Course of theoretical physics (Elsevier, 1980).
[21] J. D. Stokes, H. P. Dahal, A. V. Balatsky, and K. S. Bedell, Philosophical Magazine Letters **93**, 672 (2013).
[22] R. Saito, G. Dresselhaus, and M. S. Dresselhaus, *Physical Properties of Carbon Nanotubes* (World Scientific Publishing, 1998).
[23] C. L. Kane and M. P. A. Fisher, Phys. Rev. Lett. **68**, 1220 (1992).